Dean&Francis

ISSN 2959-6157

EHR Forecasting via Implicit Neural ODEs

Yulin Ji

Abstract:

The widespread adoption of Electronic Health Record (EHR) systems has generated vast repositories of valuable clinical data. Utilizing this information enables the development of predictive methods for proactive healthcare, enhanced medical services, and optimized resource allocation.This study employs the MIMIC-IV dataset to address challenges in generating actionable insights from longitudinal EHR data. We introduce a novel model based on Implicit Neural Ordinary Differential Equations (Neural ODEs), focusing on predicting Length of Stay (LoS) and In-Hospital Mortality (IHM). The model first encodes multimodal clinical codes into a low-dimensional space via a clinical embedding module, mitigating noise from heterogeneous data. An implicit Neural ODE network then captures the temporal dynamics of vital signs and lab results for efficient continuous-time modeling, The key experimental results show that the AUC of the proposed model in the prediction of hospital stay reaches 0.81, and the accuracy reaches 97%, which is 12% and 9% higher than that of the baseline model, respectively. In terms of mortality prediction, it also showed advantages, with AUC reaching 0.785 and mean square error decreasing from 0.0084 to 0.0036, a decrease of about 39.5%, which was significantly better than the prediction effect of the baseline model.

Keywords: Electronic Health Records, Neural Ordinary Differential Equations, Clinical Embedding, MIMIC-IV, Clinical Prediction

I, INTRODUCTION

Emerging in the late 20th century, Electronic Health Records (EHRs) have evolved significantly over decades, driven by technological innovation and policy support. Today, EHRs are globally adopted as core tools for enhancing patient safety, optimizing hospital operations, and securely storing medical information. They systematically document patient diseases, diagnoses, treatments, nursing care, and referrals, providing a comprehensive, real-time health overview for clinical decision-making. This enables more precise diagnoses and alleviates pressure on medical resources.

The widespread implementation of EHRs has generated vast volumes of timestamped clinical data, creat-

ISSN 2959-6157

ing unprecedented opportunities for clinical decision support and patient management[1]. Developed countries like the US, benefiting from favorable foundations, achieved early milestones and established regional EHR systems. In China, EHR development progressed from paper-based to structured and fully electronic systems, guided by national policies, funding, and technological leadership. Initiated in 1995 under the Ministry of Health's "Golden Medical Project" (including Military Projects 1-3), theoretical exploration and small-scale EHR trials began. By 2021, nearly half of China's provinces achieved EHR adoption rates exceeding 90%.besides Deep learning is widely applied to EHRs, primarily for Information Extraction: Including concept, temporal, and relation extraction. *Example:* Y. Lv et al. combined medical concept mapping, autoencoders, and standard text preprocessing to feed features into a Conditional Random Field (CRF) classifier, significantly improving extraction efficiency.The second outcome Prediction: Such as length of stay and mortality prediction. *Example:* Choi et al.›s Doctor AI architecture uses GRUs trained on clinical events and timestamps to simulate physician behavior, predicting future diagnoses or the next coded event the knowledge graph of electronic health records(see Fig1).

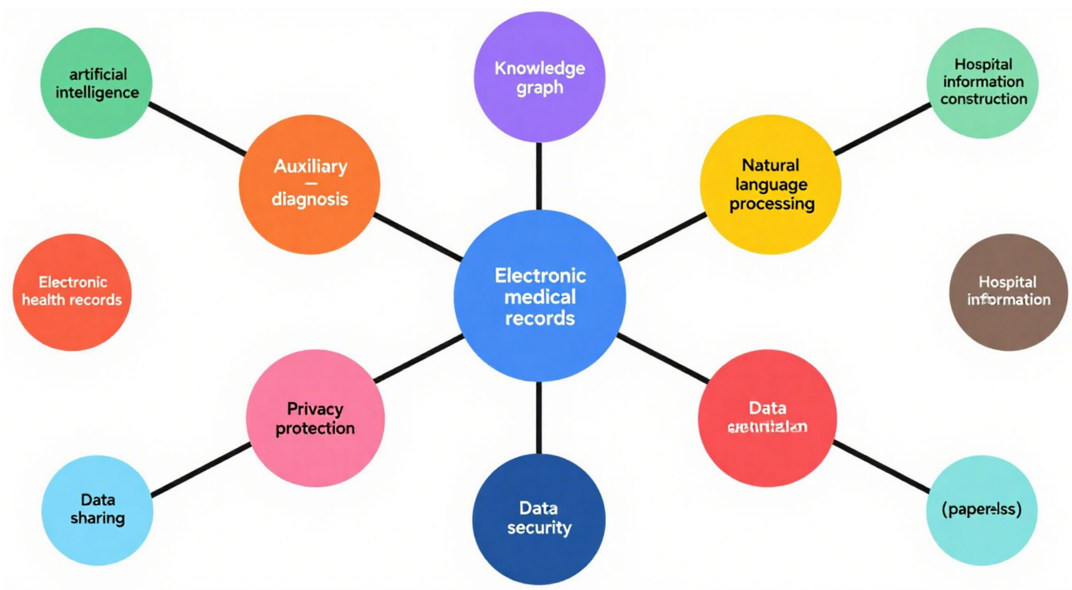

Figure 1.Knowledge Graph of Electronic Health Records

II, RELATED WORK

A, *Neural Ordinary Differential Equations*

Neural Ordinary Differential Equations (NODE)[2] is a model architecture proposed by Chen et al. in 2018 that introduces continuous-time dynamical systems into deep learning. Compared to discrete layer structures, Neural ODEs[3] can naturally model temporal continuity, making them well-suited for time-series data. In the medical field, they are particularly applicable for modeling time series and individualized health trajectories, such as disease progression[4], length of hospital stay prediction, and mortality prediction. The derivative function of the hidden layer is modeled using a neural network. It is assumed that each patient is described by a time-continuous[5] hidden state with a dimension. The temporal[6] evolution is modeled using a system of Neural Ordinary Differential Equations:

$$\frac{dh(t)}{dt} = f_d\left(h(t);\theta_d\right) \tag{1}$$

where is $f_d\colon \mathbb{R}^{d_h} \mapsto \mathbb{R}^{d_h}$ a parameterized dynamics function, and θ is a vector of learnable parameters. To evolve the hidden state from time stamp t_0 to t_1, the following Initial Value Problem (IVP) is considered:

$$h(t_1) = h(t_0) + \int_{t_0}^{t_1} f_d\left(h(t);\theta_d\right)dt \tag{2}$$

$$h(t_k) = IVPSolve\left(f_d, \theta_d, h(t_{k-1})\right), [t_{k-1}, t_k]) + \epsilon \tag{3}$$

where ϵ represents numerical approximation error. The model can learn to predict diagnostic codes at future time points from the patient's state.

B, Clinical Embedding Module

Electronic Health Records (EHRs) contain patients› medical events recorded as long-term, discontinuous time series. The implicit temporal relationships within these patterns carry rich clinical and pathological information, providing crucial sequential feature support for building predictive models of hospital length of stay and mortality risk.

Medical concept embedding is a feature extraction method that transforms a set of timestamped medical concepts into vectors, which are then fed into supervised learning algorithms. The quality of these embeddings largely determines the learning performance on healthcare data.

Traditionally, one-hot encoding[7][8][9] used in the medical domain maps clinical concepts to high-dimensional, sparse binary vectors, suffering from the curse of dimensionality. Inspired by distributed semantic representation theory, continuous vector learning methods based on word embeddings can effectively capture latent semantic relationships between medical concepts,generating low-dimensional dense representations rich in semantic information[10][11][12][13][14][15][16]. This representation paradigm has been successfully applied to the representation learning layers of medical AI models, significantly improving generalization capabilities for clinical prediction tasks.

Let $\mathcal{C}$ denote the set of possible clinical codes with cardinality $C=|\mathcal{C}|$. The goal of embedding is to find a transformation that maps a set of clinical codes to a fixed-size vector representation. This provides a compact encoding while preserving high informational content about the clinical codes.

$$g = f_M\left(v;\theta_M\right) = W_M v + b_M \tag{4}$$

W_M a learnable matrix, b_M a learnable vector, θ_M is Concatenation operation.

The alternative approach is Graph-based Attention Model (GRAM) embedding. Several widely-used clinical coding systems, such as SNOMED-CT and ICD, can be organized into a medical ontology–a hierarchical structure of codes where higher-level codes represent abstract medical concepts, while descendant codes at lower hierarchy levels denote increasingly specific and precisely defined medical concepts. Mathematically, this hierarchy is represented as a directed acyclic graph (DAG),In the GRAM algorithm, each medical concept is encoded as a convex combination of “base embeddings” corresponding to the code itself and all its ancestors. This approach enriches embeddings by preserving information about code ancestry, while mitigating overfitting risks for rare medical concepts in training datasets. The specific procedure is detailed below:

$$g_i = \sum_{j\in\mathcal{A}(i)} \alpha_{ij} e_j,\ \sum_{j\in\mathcal{A}(i)} \alpha_{ij} = 1, \alpha_{ij} \geqslant 0 \tag{5}$$

$$\alpha_{ij} = \frac{exp\left(f_R\left(e_i,e_j\right)\right)}{\sum_{k\in\mathcal{A}(i)} exp\left(f_R\left(e_i,e_k\right)\right)} \tag{6}$$

$$f_R\left(e_i,e_j;\theta_R\right) = u_R^T tanh\left(W_R\begin{bmatrix} e_i \\ e_j \end{bmatrix} + b_R\right) \tag{7}$$

$$G_{(\theta_E,\theta_R)} = \left[g_1;\ldots;g_C\right] \in \mathbb{R}^{C\times d_e} \tag{8}$$

$$g = f_G\left(v;\theta_E,\theta_R\right) = tanh\left(vG_{(\theta_E,\theta_G)}\right) \tag{9}$$

Clinical embedding modules play a pivotal role in Electronic Health Records (EHRs), transforming high-dimensional, sparse medical codes (e.g., ICD or SNOMED) into dense vector representations for efficient downstream model processing. By converting multi-hot encoded representations of clinical encounters into embedding vectors, models can capture latent relationships among clinical events such as diagnoses, treatments, and laboratory tests.

III, Materials and Methods

A, CEM-LNODE Model

With the advancement of medical informatization, Electronic Health Records (EHRs) have become a critical data source documenting patients’ diagnostic and treatment trajectories. EHRs contain structured clinical codes (e.g., diagnoses, laboratory tests, treatments) and irregularly-sampled medical encounters characterized by high-dimensional sparsity, irregular temporal sampling, and complex temporal dynamics, posing significant challenges for healthcare modeling.To comprehend patient state evolution and predict length of hospital stay and mortality risk based on admission disease status, this paper proposes a Clinical Embedding Module-based Latent Neural Ordinary Differential Equations model (CEM-LNODE). By integrating latent neural ODEs with a clinical embedding module, we establish a unified and robust framework for disease risk modeling. The dynamic modeling architecture is illustrated in Figure 2.

ISSN 2959-6157

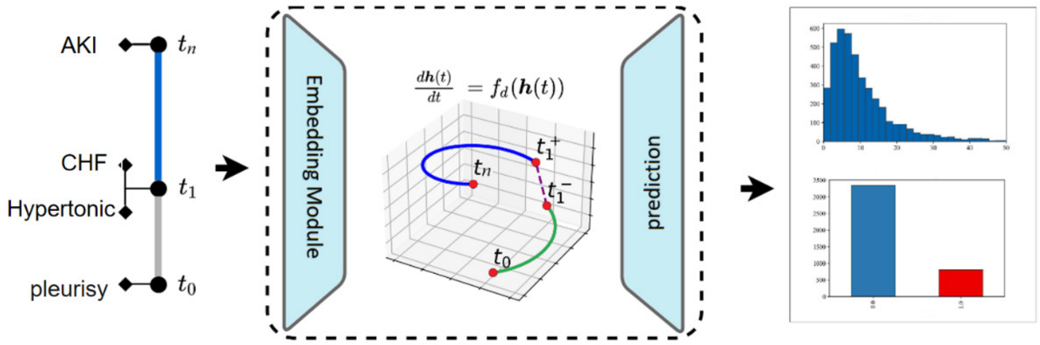

Figure 2. dynamic modeling architecture

The Implicit Neural ODE Model processes Electronic Health Records (EHRs) with continuous timestamps $\{t_0,t_1,\ldots t_n\}$ It first converts discrete medical diagnostic labels (such as "Acute Renal Failure" and "Congestive Heart Failure") into low-dimensional dense vector representations via a clinical embedding module, combining them with timestamp markers to form a time-series input. Subsequently, it employs differential equations to model the continuous dynamic evolution of hidden states, capturing the changing patterns of medical concepts over time. Finally, it generates predictions for length of stay and mortality risk based on the dynamically evolved state information. This end-to-end process integrates the semantic encoding of discrete diagnoses with continuous-time dynamic modeling, enabling comprehensive analysis and prediction of medical time-series data. Figure 3 shows the framework diagram of the model.

Based on the model framework diagram, this model integrates the expressive power of clinical embeddings with the generative modeling capabilities of the latent neural ODE. Through the latent variable trajectories learned via joint training, it can more accurately predict patient outcomes such as length of stay and mortality risk. The model primarily consists of four components: an initialization module, an encoder, a decoder, and a state updater

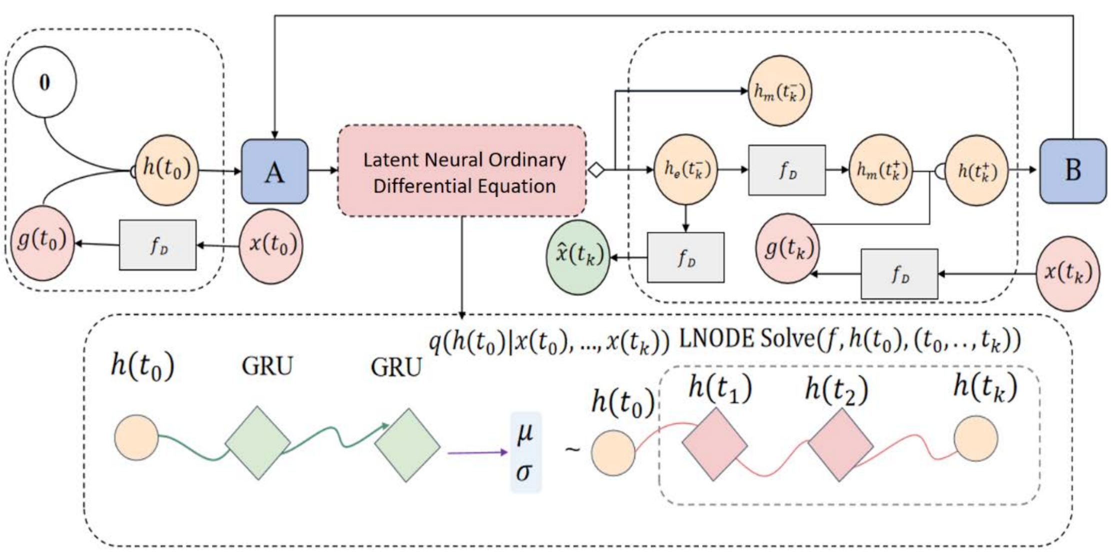

Figure 3. CEM-LNODE model

This model employs Neural Ordinary Differential Equations (Neural ODEs) and a Recurrent Neural Network (RNN) as the encoder. The Recurrent Neural Network (RNN) is[17][18][19] a traditional neural network capable of processing time-series data and storing historical information. It utilizes predictions from previous historical information as contextual signals to improve decision-making for future timesteps, as represented by the recurrent relationship shown in Figure 4,and Equation 11.

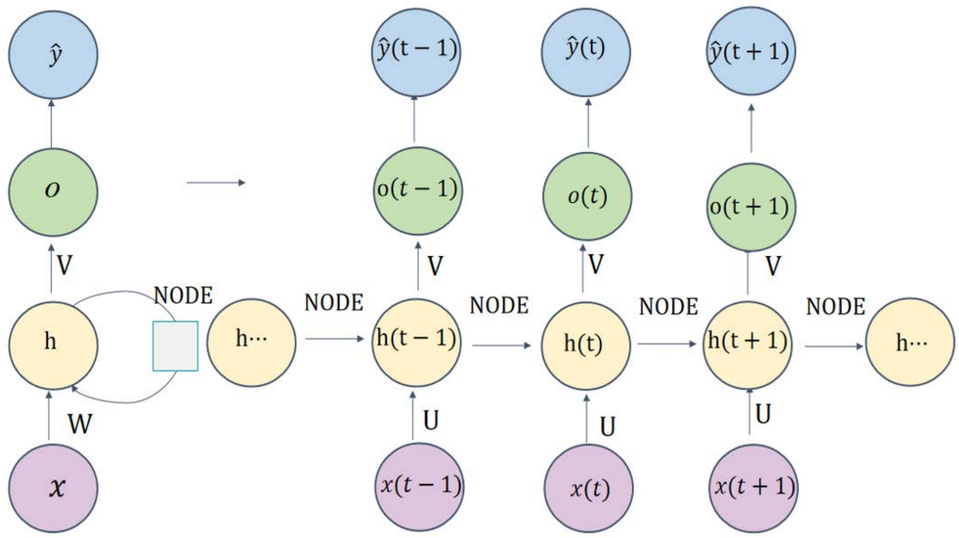

Figure 4. RNN Encoder

$$y(t)=f\left(y(t-1),x(t),t\right) \quad (10)$$

while the numerical solution of the Neural Ordinary Differential Equation is shown in Equation 12:

$$x(t+g)=x(t)+gf\left(x(t),t\right) \quad (11)$$

The decoder employs a Neural Ordinary Differential Equation (Neural ODE) because it can explicitly decouple system dynamics, enabling both forward and reverse integration for predictions. The latent variable trajectory refers to the continuous temporal evolution of latent states modeled by the Neural ODE, where the latent variable $h(t_i)$ is no longer a static vector but a time-dependent dynamical system, as illustrated in Figure 5

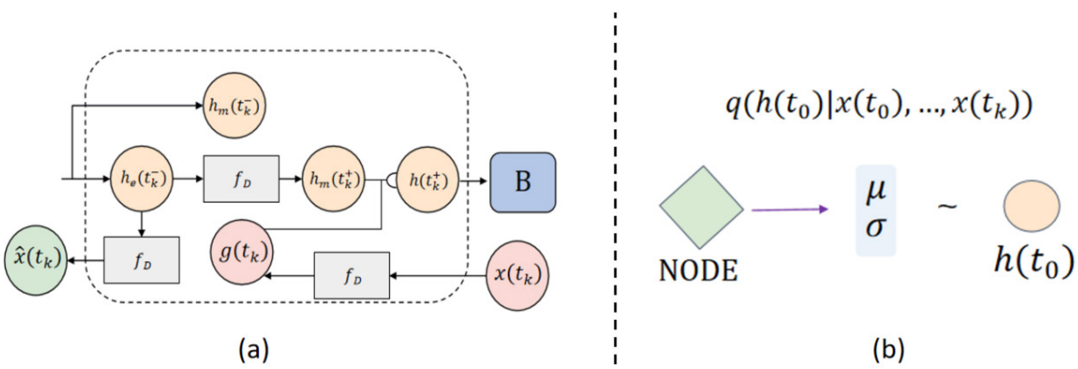

Figure5. More detail in Decoder

$$h(t_1),h(t_2),..h(t_N)=LNODESolve\left(h(t_0),f,\theta_f,t_0,t_1,\ldots,t_N\right) \quad (12)$$

$$\frac{\partial h(t_i)}{\partial t}=f(h(t),\theta_f) \quad (13)$$

$$x_{t_i}\ p\left(x\mid h(t_i),\theta_x\right) \quad (14)$$

Status updates Equation 16:

$$h(t_1^-)=\begin{bmatrix} h_m(t_1^-) \\ h_e(t_1^-) \end{bmatrix}=IVPSolve\left(f_d,\theta_d,h(t_0),[t_0,t_1]\right) \quad (15)$$

The CEM-LNODE model is a hybrid framework specifically designed for healthcare scenarios. It addresses the analysis and prediction of irregularly sampled medical time-series data by integrating discrete clinical semantics with continuous-time dynamic modeling. The core architecture combines a Clinical Embedding Module (CEM) with a Latent Neural Ordinary Differential Equation (LNODE). The former encodes discrete medical diagnostic labels (e.g., 'acute renal failure,' 'congestive heart failure') into low-dimensional dense vectors, capturing semantic relationships among diseases. The latter employs a latent ordinary differential equation (ODE) model combine with diffusion model[20][21][22], leveraging numerical solvers to process irregularly sampled time-series data.

The algorithmic workflow begins with probabilistic generation of initial states. It then simulates long-term

ISSN 2959-6157

dependencies in hidden states through the ODE-based dynamical system, while incorporating a memory update mechanism that integrates real-time inputs with historical states when decoding observations. This ultimately generates predictions for hospital length of stay and mortality risk.
Within the medical domain, this model's development trend highlights its enhanced capacity for deep analysis of complex healthcare data. On one hand, its continuous-time modeling intrinsically aligns with the non-uniformly spaced monitoring data inherent in clinical settings.

IV, EXPERIMENTS

MIMIC-IV (Medical Information Mart for Intensive Care) comprises electronic health records of over 256,000 patients who received intensive care or emergency department services at Beth Israel Deaconess Medical Center (BIDMC) in Boston, Massachusetts, USA between 2008 and 2019. This dataset captures comprehensive hospitalization details for each patient, including clinical data such as laboratory measurements, medication administration records, and vital signs. It encompasses more than 257,000 unique patients, constituting 524,000 hospital admissions. MIMIC-IV utilizes the ICD-10 coding system, which is mapped to ICD-9 and ultimately to the CCS coding scheme.
The MIMIC-IV dataset adopts a modular architecture reflecting data sources. Our research pipeline utilizes two core modules: ICU (Intensive Care Unit) and Hosp (Hospitalization), containing fundamental hospitalization information, ICU-level data, and hospital-level data respectively. Its data architecture is structured according to clinical workflows as follows:

Table 1

Clinicalbusiness domains	Key data sheets	Data characteristics
Clinical business	patients admissions transfers	basic information of the patient; Hospitalization records, recording the patient's admission information; Ward metastasis records
Laboratory inspection	labevents d_labitems(	Contains serology, biochemistry and other test results and metadata
Microbiological testing	microbiologyevents d_micro(microbiology Codebook)	Microbiological data such as pathogen culture and susceptibility testing were recorded
Doctor'sorder management	poe(The doctor's order is recorded) poe_detail	Reflect the examination/treatment instructions issued by the doctor and the status of implementation
Medication Management	emar emar_detail prescriptions pharmacy	Closed-loop records of the whole process from the issuance of medical orders to drug administration
healthcare costs	diagnoses_icd d_icd_diagnoses(ICD Codebook1) procedures_icd(ICD Codebook2) d_icd_procedures(ICD Codebook3) hcpcsevents(HCPCS Code) d_hcpcs(HCPCS Codebook) drgcodes(	Medical behavior codes based on international classification standards and Cost correlation data
Clinical services Record	services	Record information on specialist services (e.g., consultation, referral) received by patients

I, Data processing

In the processing of the MIMIC-IV dataset, some data that is not relevant to this prediction is removed to prevent interference with the data, such as outpatients, who usually only come to the hospital for some mild illness (cold, headache, etc.). Some patients come for repeated consultations, and will default to the last one and delete the previous visit record.

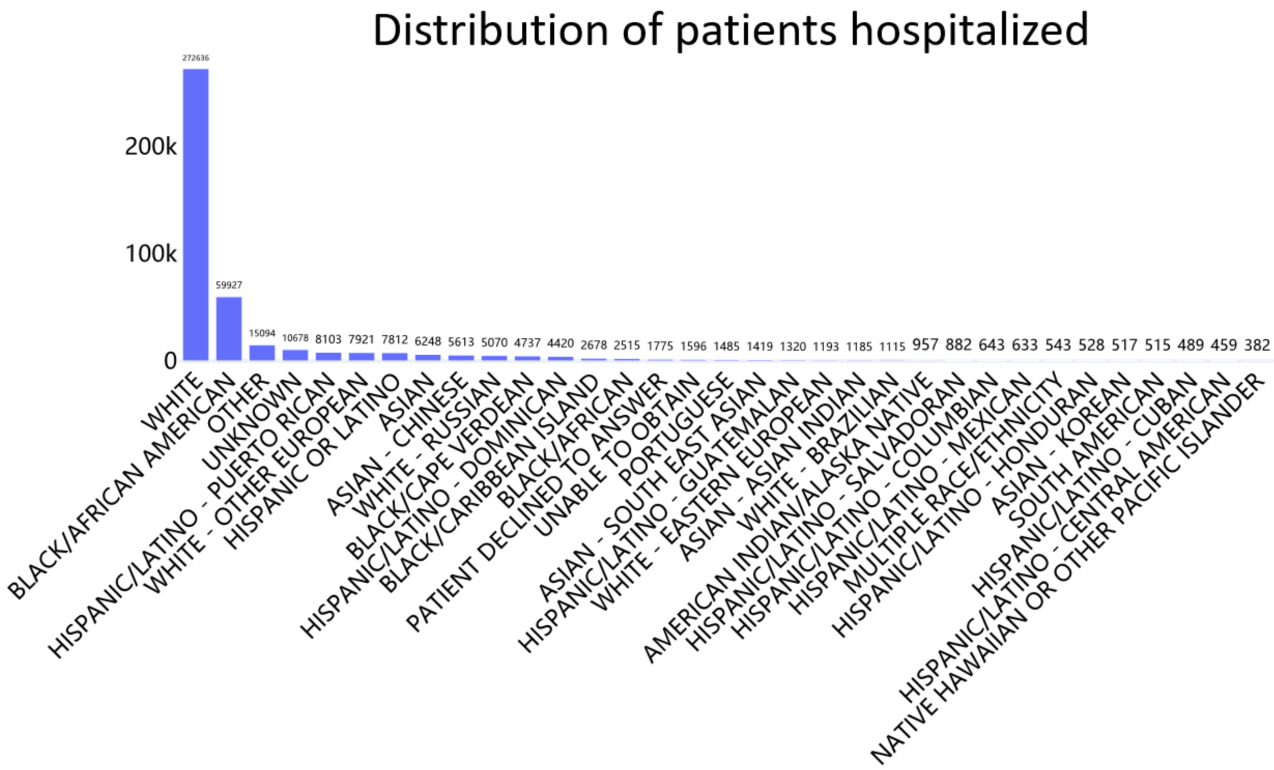

Figure6 .Distribution map of patient hospitalization

Due to the excessive and mixed races, this paper divides the data according to race, and only the first five columns are discussed. The types of patient hospitalization are divided into emergency admission, observation unit observation, observation to formal admission, emergency admission, day surgery admission, direct observation, elective planned admission, and date observation visit.

The age of the patient is also an important factor affecting the length of hospitalization, but the age distribution is too wide, so this paper divides the data according to 20 age groups and plots Figure 8.Too much table data will slow down the data reading speed, and integrating in one table will increase the speed of reading data, and can also speed up the model running, so different Excel tables are integrated through the same SUBJECT_ID, and some unnecessary columns (such as insurance, gender, etc.) are deleted, and some important information (such as whether to enter the ICU, whether to be in the neurosurgical intensive care unit, etc.) is added to the table.

ISSN 2959-6157

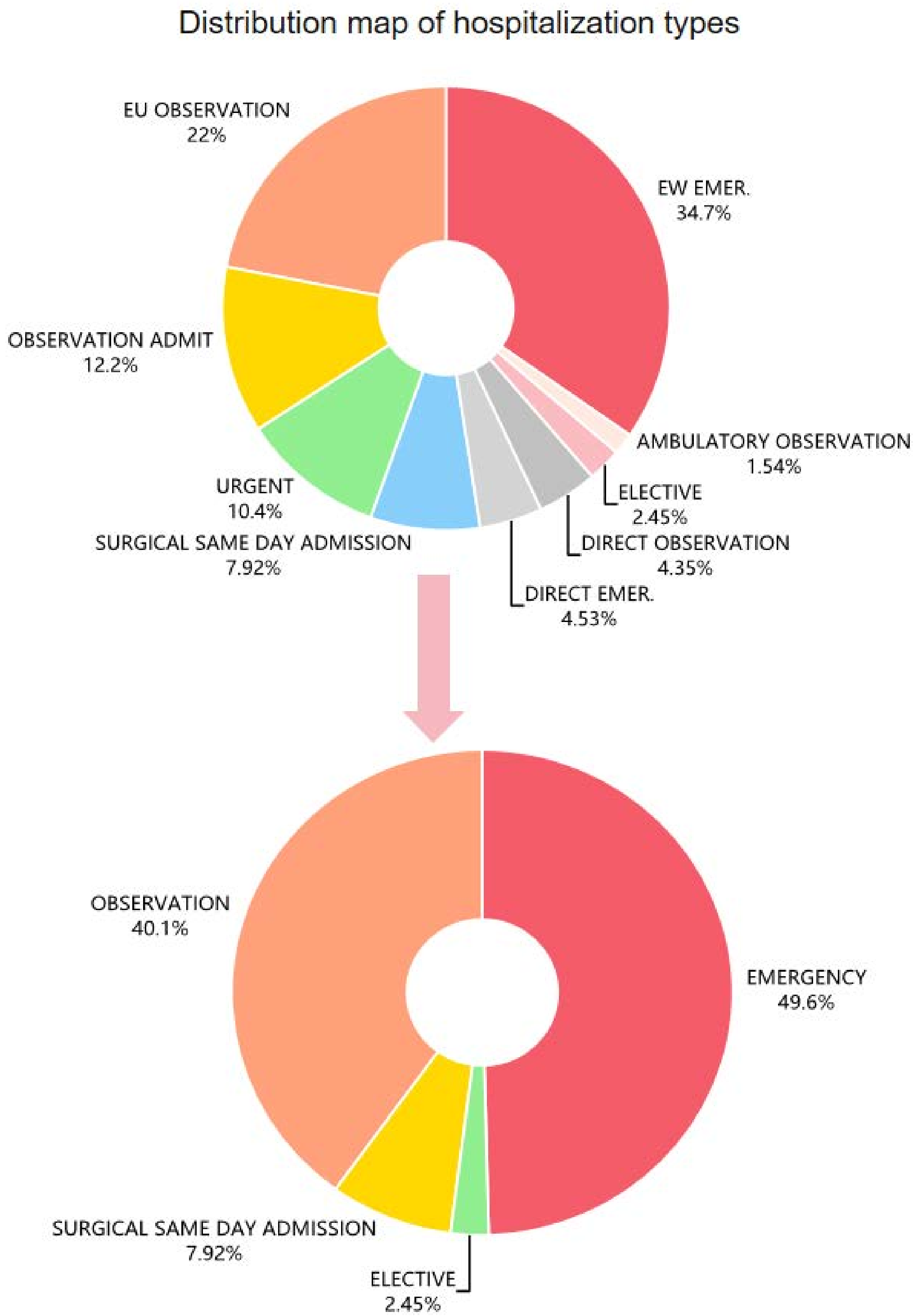

Figure7 . Distribution map of hospitalization types

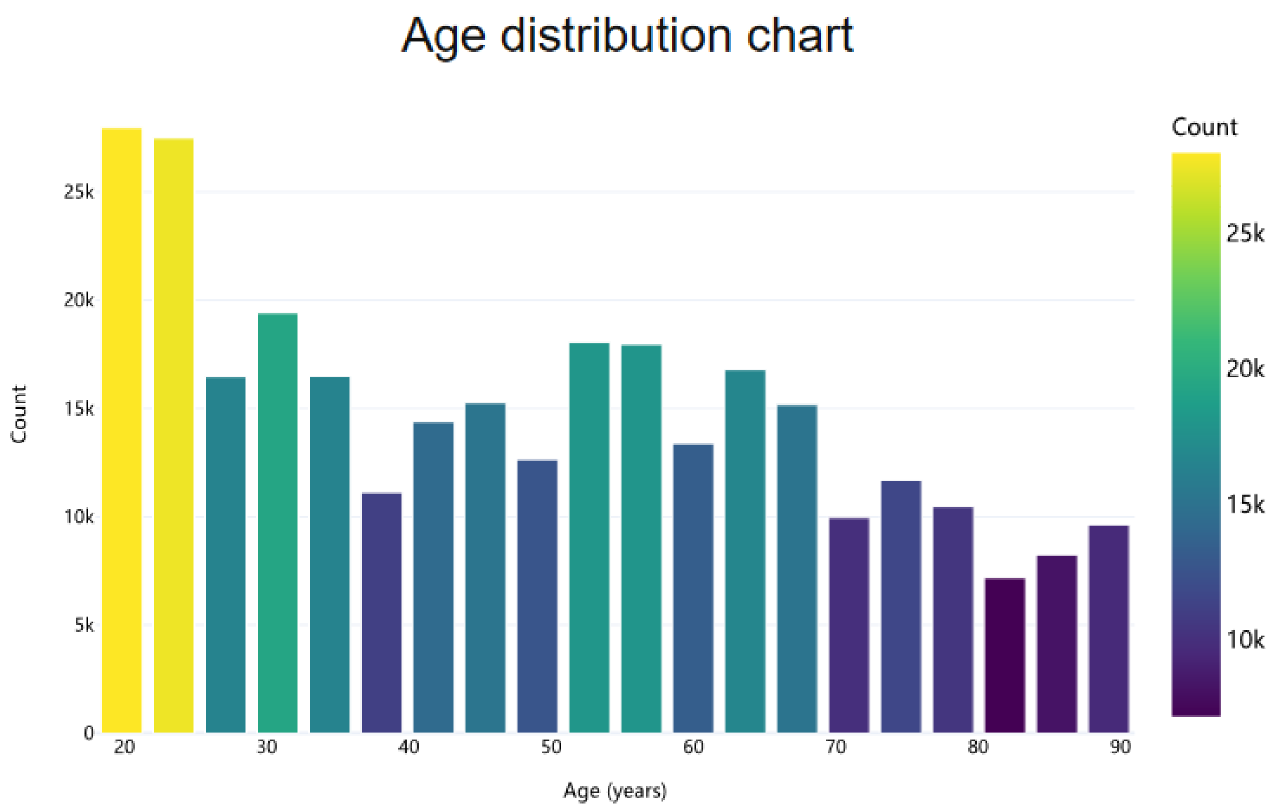

Figure8 . Age distribution chart

In addition, the Pearson Correlation Coefficient can reflect the relationship between various variables, with values ranging from $[-1,1]$. The closer the value is to 1, the stronger the correlation between them, as shown in Figure 9.

ISSN 2959-6157

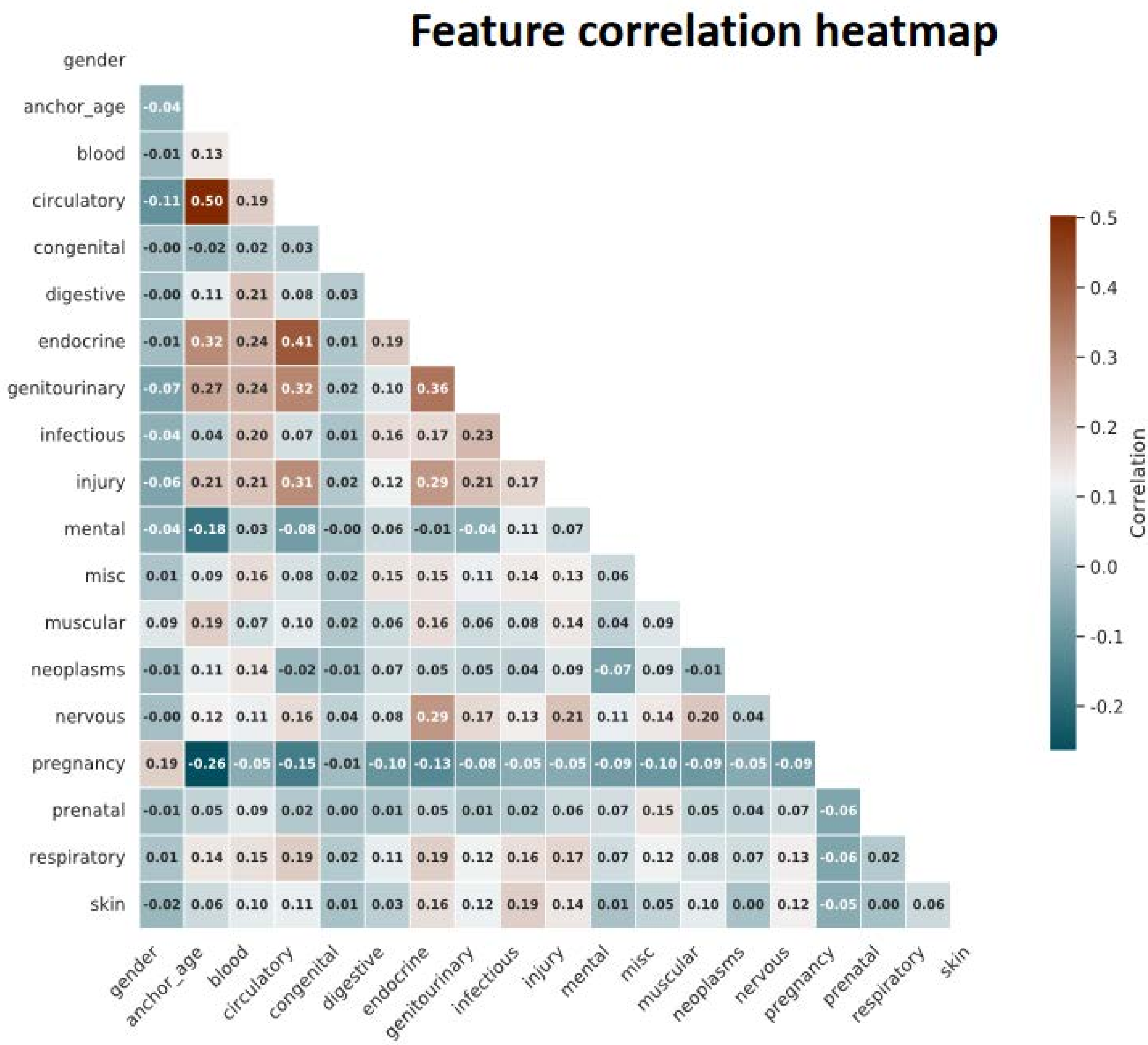

Figure9. Feature correlation heatmap

II, Model performance evaluation index

In the prediction of length of hospital stays and mortality for electronic health records, it is crucial to comprehensively evaluate the performance of the model. In order to accurately grasp the prediction ability, generalization and stability of the model, multiple evaluation indicators need to be used for comprehensive consideration in the experiment.

$$Accuracy = \frac{TP+TN}{TP+FP+TN+FN} \tag{16}$$

$$Recall = \frac{TP}{TP+FN} \tag{17}$$

$$Precision = \frac{TP}{TP+Fp} \tag{18}$$

$$F1-Score = 2 \cdot \frac{Precision \cdot Recall}{Precision + Recall} \tag{19}$$

$$\mathbb{D}_{KL}(P \| Q) = \int_{-\infty}^{\infty} p(x) ln\left(\frac{p(x)}{q(x)}\right) dx \tag{20}$$

$$q(z_0 \mid x) = N(\mu, diag(\sigma^2)) \tag{21}$$

$$p(z_0) = N(0, I) \tag{22}$$

$$KLfp = \mathbb{D}_{KL}(q(z_0 \mid x) \| p(z_0)) \tag{23}$$

$$FP_{STD} = \sqrt{\frac{1}{d}\sum_{i=1}^{d}\sigma_i} \tag{24}$$

Among them, TP, TN, FP, and FN represent true positives, true negatives, false positives, and false negatives, respectively. TP is the correct classification of the positive category, the correct classification of the negative category is written as TN, FP is the false prediction of positive values, and FN is the false prediction of negative values. Accuracy reflects the proportion of the number of samples correctly classified by the model to the total number of samples, and is a visual index to evaluate the overall performance of the model, as shown in Equation 23. However, in the case of uneven data distribution, the accuracy may be biased, so it needs to be considered in combination with other indicators.

Recall, also known as sensitivity, represents the model's ability to successfully identify all true predicted hospital days, as shown in Equation 24. High recall indicates high coverage of true positive categories. The experiment also uses an F1-Score, with a higher F1 score meaning that the model performs better in both accuracy and coverage, as shown in Equation 26. The ROC curve and its underlying area (AUC) are also important indicators to evaluate the performance of the classification model. The ROC curve shows the relationship between the true positive rate and the false positive rate of the model at different thresholds, and the closer the AUC value is to 1, the better the classification effect of the model.

A confusion matrix is a specific table layout used to visualize the performance of supervised learning algorithms, particularly classification algorithms. In this matrix, each row represents the actual category and each column represents the predicted category. Each cell of the matrix contains the number of samples under that actual and predicted categories. The confusion matrix provides a more comprehensive understanding of the model's performance across different categories.

V, Results

Comparisons and benchmarks were made against state-of-the-art baseline methods, and the baseline methods considered were:

RNN: A classical recurrent neural network model that specializes in processing sequence data, with the core idea of capturing temporal dependencies in sequences through a recurrent structure.

NODE-RNN: An innovative model that combines neural ordinary differential equations with recurrent neural network frameworks. The core of this study is to transform the discrete hidden state update process in the traditional recurrent neural network into a continuous time differential equation, and dynamically solve the evolution trajectory of the hidden state through numerical integration methods.

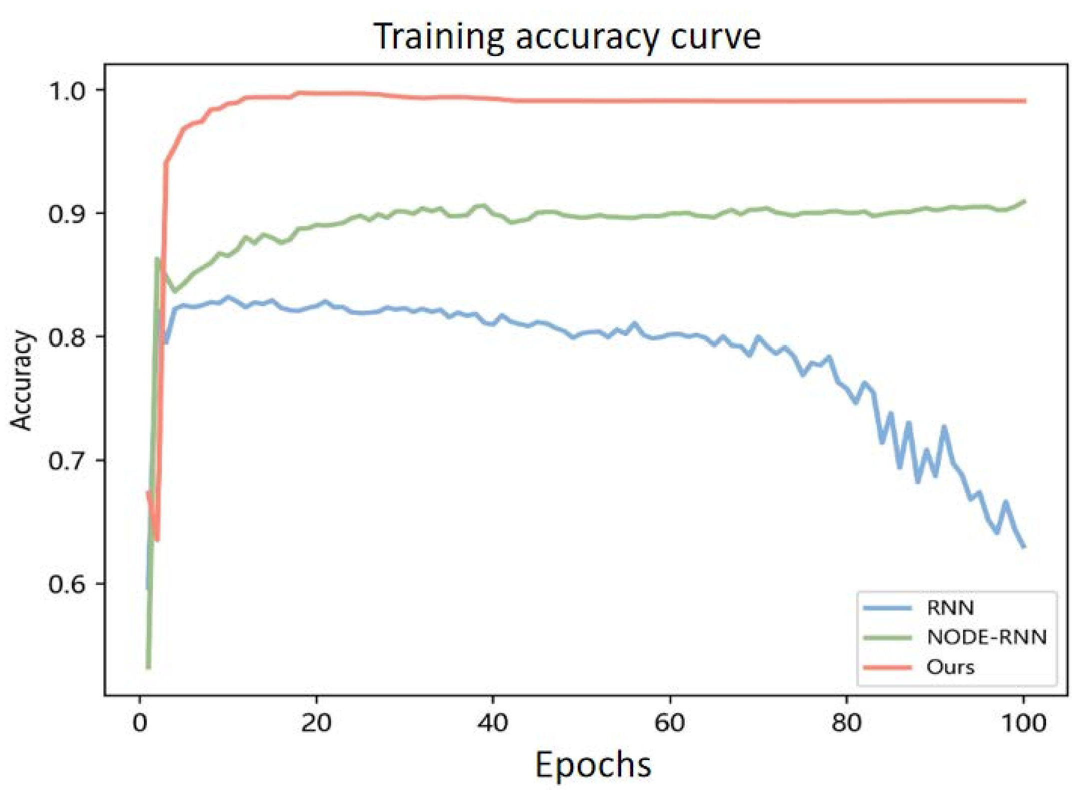

Figure10. Training accuracy curve

ISSN 2959-6157

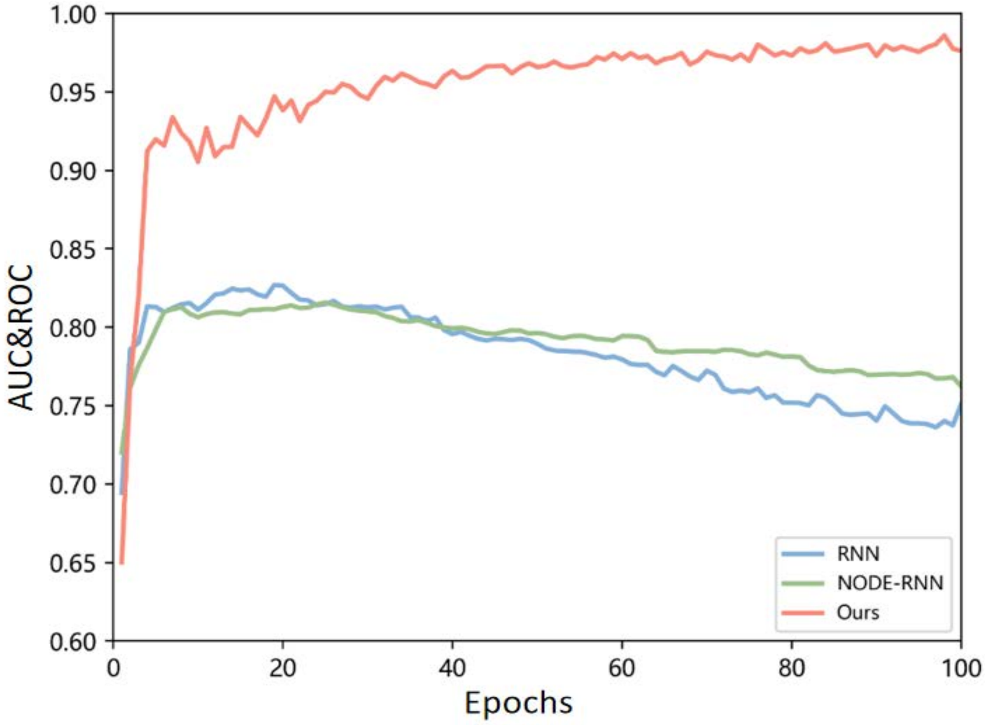

Figure11. AUC comparison chart of RNN, NODE-RNN, CEM-LNODE

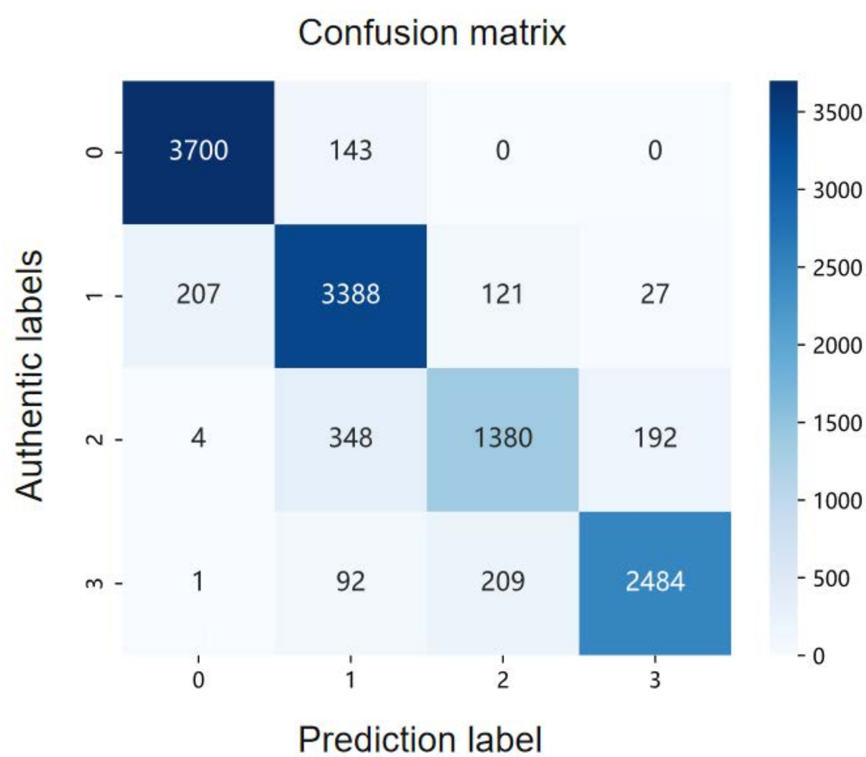

Figure12. Confusion matrix for predicting length of hospital stay

The above figure is a comparison of the AUC of the three models. As can be seen from the graph, the AUC value of the CEM-LNODE model rises rapidly at the beginning of the test, and then flattens after about 10-20 epochs, and finally converges to a maximum value (close to 1). This indicates that the model can quickly capture most of the information in the data at the beginning of the test, and the final AUC performance is slightly better than that of RNN and NODE-RNN models, indicating that the CEM-LNODE model may have stronger expression capabilities, especially when dealing with complex features.

In addition to producing accurate predictions, the model can also generate interpretive results suitable for visualization. Figure 12 provides a visualization of the length of hospital stay. In this paper, 0-10 days are regarded as short-term (0), 0-20 days as medium-term (1), 0-30 days as medium-term (2), and 30 days after (3). As can be seen from the figure, basically the results of the model's predictions are correct, except for a few predictions that are a bit wrong in the medium term. Figure 11 records the comparison between the predicted value and the real value, and the predicted value and the real value fit very well throughout the process, which shows that the prediction result is very correct.

VI, DISCUSSION AND LIMITATIONS

This paper analyzes and proposes a prediction method based on the implicit god frequent differential equation model (CEM-LNODE) from the perspective of electronic health records. The CEM-LNODE model predicted the length of hospital stay and mortality of hospitalized patients, respectively, and was validated on the MIMIC-IV. dataset. The Shen Frequent Differential Equation has the advantages of constant memory consumption (memory usage is only related to the dimension of input and output), natural adaptation to continuous dynamic and irregular sampling data (accepting observation data at any time point and output state at any time point), and interpretability (analyzing the evolution process through trajectory analysis), which improves the prediction of hospital stay and mortality. The clinical embedding module solves the problem of both vector dimension explosion and data sparsity of traditional single-thermal coding methods, and can solve the problem of high noise in MIMIC-IV datasets.

In this paper, the performance of CEM-LNODE and multiple baseline models on MIMIC-IV is compared, and the results show that CEM-LNODE performs better in terms of both hospital stay and mortality prediction. In addition, it has a stronger generalization ability on different datasets. CEM-LNODEs do not require discrete observation time or input data as a preprocessing step, making them suitable for irregularly sampled time series data that are common in many applications.

V, REFERENCES

[1] Esteban C ,Staeck O ,Yang Y , et al.Predicting Clinical Events by Combining Static and Dynamic Information Using Recurrent Neural Networks.[J].CoRR,2016,abs/1602.02685

[2] Xinbo L ,Yi G ,Jinfeng Y , et al.Clinical Relation Extraction with Deep Learning[J].International Journal of Hybrid Information Technology,2016,9(7):237-248

[3] GoldR ,GunnR ,Owens–JaseyC , et al.Health center strategies to document and track social needs referrals in the EHR[J].Health Services Research,2025,60(S1):e14525-e14525.

[4] Li J ,Liu D ,Ma G , et al.DBFF-GRU: dual-branch temporal feature fusion network with fast GRU for multivariate time series forecasting[J].Applied Intelligence,2025,55(7):622-622.

[5] Xie Y ,Yan Y ,Hong Q , et al.Heterogeneous treatment effects of stress ulcer prophylaxis among ICU patients at risk for gastrointestinal bleeding[J].BMC Medicine,2025,23(1):206-206.

[6] Pandey G ,Ghanekar U .Convolutional Neural Network-Based Framework for Single Image Superresolution of Magnetic Resonance Imaging Images Using Multiscale Feature Extraction and Attention Mechanism[J].Pattern Recognition and Image Analysis,2025,35(1):31-43.

[7] Liao H ,Chen Y ,Chen D , et al.Hierarchical fine-grained state-aware graph attention network for dialogue state tracking[J].The Journal of Supercomputing,2025,81(5):671-671.

[8] Anonymous .MBL Partners with RTDC To Commercialize Discoveries[J].Sea Technology,2009,50(10):63.

[9] Shen Y ,Lin K ,Yang L , et al.Association between the lactate dehydrogenase-to-albumin ratio and 28-day mortality in septic patients with malignancies: analysis of the MIMIC-IV database[J].BMC Cancer,2025,25(1):637-637.

[10] Budkina M E ,Kuznetsov B E ,Lazovskaya V T , et al.Neural network approach to intricate problems solving for ordinary differential equations[J].Optical Memory and Neural Networks,2017,26(2):96-109.

[11] Isazade V ,Qasimi B A ,Namivandi S M , et al.Landslide Susceptibility Assessment Using Recurrent Neural Network (RNN)—A Case of Chabahar and Konarak in Iran[J].Indian Geotechnical Journal,2025,(prepublish):1-21.

[12] Coelho C ,Costa P F M ,Ferrás L .Enhancing continuous time series modelling with a latent ODE-LSTM approach[J]. Applied Mathematics and Computation,2024,475128727-.

[13] Angelos K, Apoorv V, Nikolaos P, Francois F, et al. Transformers Are RNNs: Fast Autoregressive Transformers with Linear Attention[C], International Conference on Machine Learning, 2020, 119

[14] Alex Sherstinsky. Fundamentals of Recurrent Neural Network (RNN) and Long Short-Term Memory (LSTM) Network[J], Physica D: Nonlinear Phenomena, 2020, 404

[15] Karita S, Chen N, Hayashi T, Hori T, Inaguma H, Jiang Z, Someki M, Soplin N E Y, Yamamoto R, Wang X, Watanabe S, Yoshimura T, Zhang W, et al. A Comparative Study on

ISSN 2959-6157

Transformer vs RNN in Speech Applications[J], 2019 IEEE Automatic Speech Recognition and Understanding Workshop (ASRU), 2019: 449-456.

[16] Naoto J, Itaru K, Takeya M, Sau P W, Shinji T, Yoshihiro F, et al. Insights into the Diversification of Deep-Sea Endoparasites: Phylogenetic Relationships Within Dendrogaster (crustacea: Ascothoracida) and a New Species Description from a Western Pacific Seamount[J], Deep-Sea Research Part I: Oceanographic Research Papers, 2023, 196

[17] Noton K. Dutta, Michael L. Pinn, Petros C. Karakousis. Metformin Adjunctive Therapy Does Not Improve the Sterilizing Activity of the First-Line Antitubercular Regimen in Mice[J], Antimicrobial Agents and Chemotherapy, 2018, 62(2)

[18] Alfred B, Daisy P, Ignacio P, Michael S, Quentin M, Ozge E, Mark B, Till R, Pavel K, et al. Predation Increases Multiple Components of Microbial Diversity in Activated Sludge Communities[J], The ISME journal, 2021, 16(4): 1086-1094.

[19] Eunice H. Pinn, Lewis Le Vay. Interpretation of the European Legal Framework for the Microbiological Classification of Bivalve Mollusc Production Areas[J], Marine policy, 2023, 148

[20] Robin R, Andreas B, Dominik L, Patrick E, Bjoern O, et al. High-Resolution Image Synthesis with Latent Diffusion Models[C], Computer Vision and Pattern Recognition, 2022, 2022(1): 10674-10685.

[21] Prafulla Dhariwal, Alexander Quinn Nichol. Diffusion Models Beat GANs on Image Synthesis[C], Conference on Neural Information Processing Systems, 2021

[22] Florinel-Alin C, Vlad H, Radu T I, Mubarak S, et al. Diffusion Models in Vision: A Survey[J], IEEE Transactions on Pattern Analysis and Machine Intelligence, 2023, 45(9): 10850-10869.